Evidence for Electron-Electron Interaction in Projectile *K*-Shell Ionization

H.-P. Hülskötter, W. E. Meyerhof, E. Dillard, and N. Guardala
Department of Physics, Stanford University, Stanford, California 94305-4060
(Received 28 July 1989)

Cross sections for projectile *K*-shell ionization were measured for 0.75–3.5-MeV/nucleon C^{5+} and O^{7+} projectiles in collisions with H_2 and He targets. The experimental results agree with plane-wave Born-approximation calculations which take into account the interaction between projectile and target electrons. We demonstrate that for energies where the target electrons have sufficient kinetic energy in the projectile frame to ionize the projectile electron, the electron-electron interaction can lead to a significant increase in the total ionization cross section.

PACS numbers: 34.50.Fa

In a collision between a projectile carrying one or more electrons and a target atom, one of the events that may occur is the ionization of a *projectile* electron. Projectile ionization is normally attributed to the Coulomb interaction between the target nucleus and projectile electron. The effect of the target electrons can be accounted for by introducing a screened Coulomb interaction between the target and the projectile electron. However, the target electrons cannot only act coherently as screening agents, but may also act incoherently as ionizing (antiscreening) agents.[1-3] In some of the literature[2,4] this has been called the "screening-antiscreening" effect. To date, there exists definite evidence only for the Coulomb interaction between the target and projectile electrons in the case of projectile inner-shell *excitation*.[5,6] Several authors have considered the influence of this interaction on target[7] and projectile[8-10] *ionization* cross sections. While some experiments[7,9] exhibit a qualitative agreement with the theoretical predictions,[2] others have not been able to confirm the interaction between target and projectile electrons. If only hydrogen and helium projectile and target collisions are used, the theoretical interpretation is made more complicated by exchange effects.[11] Here, we present a systematic study of projectile *K*-shell ionization without the latter complication and demonstrate the screening-antiscreening effect unambiguously.

In the nonrelativistic plane-wave Born approximation (PWBA), the *K*-shell ionization cross section, accounting for the effect of the target electrons, can be written as[1]

$$\sigma_K = (8\pi a_0^2/v^2)\int_0^\infty d\epsilon \sum_i \int_{q_0}^\infty (dq/q^3)\,|\langle \epsilon | e^{i\mathbf{q}\cdot\mathbf{r}} | 1s\rangle|^2 |\langle i | Z_t - e^{i\mathbf{q}\cdot\mathbf{r}} | 1s\rangle|^2 , \quad (1)$$

where v is the ion velocity, a_0 is the Bohr radius, ϵ is the kinetic energy of the ionized projectile electron, i represents the quantum numbers of the ground and excited (including continuum) states of the target atom with nuclear charge Z_t, and q is the momentum transfer, the minimum[4] of which is q_0. If the target excitation energy is small compared to the projectile ionization energy, one can apply a closure approximation,[2] which has been generalized by Anholt[4] as follows:

$$\sigma_K = (8\pi a_0^2/v^2)\int_0^\infty d\epsilon \int_{q_0}^\infty (dq/q^3)\,|F(q)|^2 S(q,Z_t) , \quad (2)$$

where $F(q) = \langle \epsilon | e^{i\mathbf{q}\cdot\mathbf{r}} | 1s\rangle$ and

$$S(q,Z_t) = [Z_t - |F_t(q,Z_t)|]^2 + \left[Z_t - \sum_j^{Z_t} |F_{jt}(q,Z_t)|^2\right]\sigma_e(E_e)/\sigma_B(E) . \quad (3)$$

Here $F_{jt} = \langle j | e^{i\mathbf{q}\cdot\mathbf{r}} | j\rangle$ is the target form factor for the jth target electron and $F_t = \sum_j F_{jt}$. E_e is the electron kinetic energy corresponding to a projectile energy of E MeV/nucleon, and σ_e is the electron-induced ionization cross section[4] taking into account threshold effects which can occur at low velocities when the target electrons do not have sufficient kinetic energy in the projectile frame to ionize the projectile electron. σ_B is the Born cross section for protons. The upper limit for the momentum-transfer integration in σ_e has to be taken as infinity so that $\sigma_e = \sigma_B$ at high velocities. The prescription gives very good agreement with the exact expression of Bates and Griffing,[1] except very close to threshold where it produces an unphysical "kink" similar to Bohr's free-electron model.[12] The two terms in Eq. (3) can be interpreted physically in terms of the ionization by a screened target nucleus and the ionization by the Z_t target electrons. The interaction between target and projectile electrons can result in an increase or a decrease of the

projectile K-shell ionization cross section. For energies below threshold the target electrons can only screen the target nucleus, thereby reducing the ionization cross section below that for a bare target nucleus. Above threshold the target electrons cannot only act as screening but also as ionizing agents. As noted in Ref. 4 for high projectile nuclear charges ($Z_p > Z_t$) the target form factors F_t and F_{jt} in Eq. (3) become very small compared to Z_t and unity, respectively. Therefore the largest relative increase in the cross section is $Z_t/(Z_t^2+Z_t)$. This is largest for $Z_t = 1$.

The ionization cross section for hydrogenlike ions in collisions with H atoms has also been calculated in the classical binary-encounter approximation (BEA).[3] Here it is assumed that the electrons and the proton collide separately with the ion. According to Ref. 3 for C^{5+} projectiles the BEA calculation agrees with the result from Eq. (3) to within a factor 1.5.

We have measured projectile K-shell ionization cross sections for collisions between C^{5+} and O^{7+} projectiles and molecular-hydrogen and helium targets. Ions in the energy range between 0.75 and 3.5 MeV/nucleon were provided by the Stanford Van de Graaff accelerator. After charge-state selection by an analyzing magnet and, if necessary, poststripping, the C^{5+} and O^{7+} projectiles were directed into a 6-cm-long differentially pumped gas cell by a switching magnet. The maximum counting rate was kept below about 1–2 kHz by tightly collimating the beam and sending it through an attenuating screen. The beam was then analyzed by electrostatic deflection plates. A detailed description of this part of the experimental setup can be found in Ref. 8. After being separated horizontally by approximately 1 cm, the different charge states were detected in two scintillator-photomultiplier counters. The ionized charge state (O^{8+} or C^{6+}) was detected in one of the counters (detector 1) while the other one (detector 2) detected the incident charge state as well as the (very weak) capture charge states. The relative detection efficiencies of the two counters were tested for each incoming ion beam and energy and were found to agree within about 3%.

For each target, the relative charge-state yields, i.e., the ratio of the number of counts in detector 1 to the sum of the counts in detectors 1 and 2, was measured at six to eight target pressures but was kept below 5%. In most cases, the relative yield without gas target was much less than 0.5%. The ratio of the number of counts in the background between the two charge-state peaks (e.g., C^{5+} and C^{6+}) to the number of counts in the incident charge state (C^{5+}) was less than 0.03%. (This estimate was obtained with a position-sensitive detector.) The K-shell ionization cross sections were then derived by least-squares fitting the background-subtracted yields as a function of the target gas pressure. This procedure is described in detail in Ref. 8. The statistical uncertainties due to the fit were generally smaller than 1%. The temperature in the experimental area was constant to 1 °C at 20 °C. The target gases used were research-grade[13] purity H_2 (99.999%) and zero-gas[13] He (99.995%) so that the total effect of impurities on the measured cross sections is below 3%. (A comparison of research-grade purity H_2 with commercial H_2 gave a 10% higher cross section for the commercial hydrogen, which agrees with the estimated effect of the impurities on the cross section.)

The biggest systematic error in the determination of the cross section arises from the effective length of the target gas cell. The entrance and exit apertures to the 6-cm-long gas cell have an area of 2 and 12 mm^2, respectively. Looking in the direction of the ion beam, the entrance aperture is preceded and the exit aperture is followed by a tube, 18-mm long with an inner diameter of 7 mm. For the pressures used here, the gas flow through these apertures and tubes is in the transitional flow regime, i.e., between viscous and molecular flow. Following the treatment of this problem in Ref. 14, we were able to calculate an effective length of our gas cell. For H_2 the result is 7.3 cm and for He it is 7.1 cm. (The

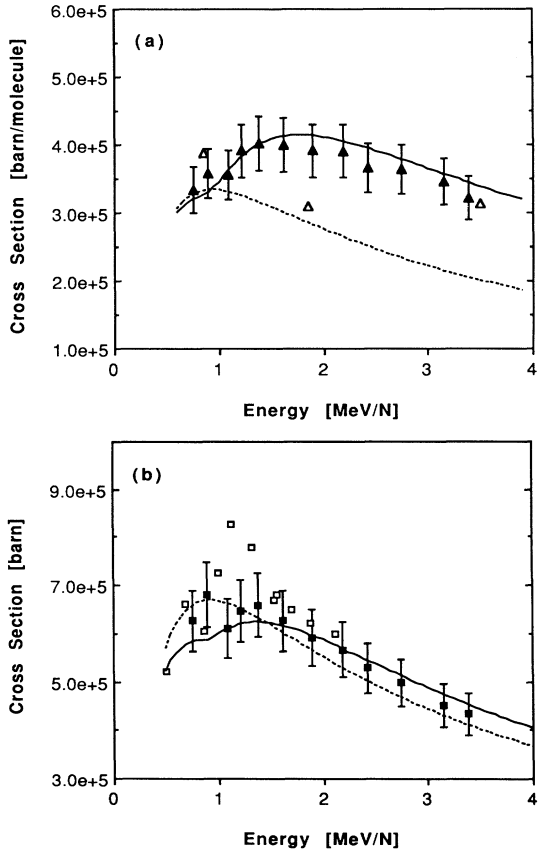

FIG. 1. Projectile ionization cross sections for C^{5+} on (a) H_2 and (b) He. Solid curves: screening-antiscreening calculations using Eq. (3); dashed curves: pure PWBA calculations. ▲, ■: this work; △: Ref. 8; □: Ref. 10. The experimental results of Refs. 8 and 10 have uncertainties of 10% to 30%.

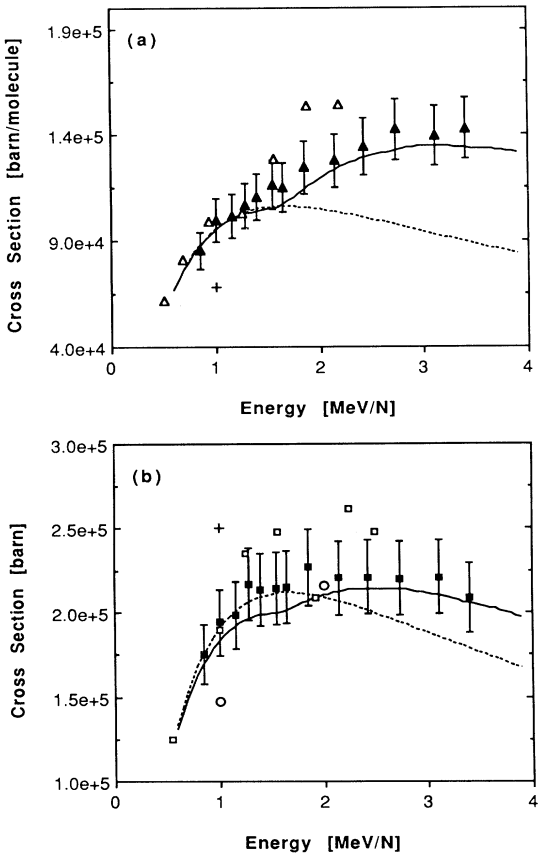

FIG. 2. Projectile ionization cross sections for O^{7+} on (a) H_2 and (b) He. Solid curves: screening-antiscreening calculations using Eq. (3); dashed curves: pure PWBA calculations. ▲, ■: this work; △,□: Ref. 10; ○: Ref. 9; +: Ref. 15. The experimental results of Refs. 9, 10, and 15 have uncertainties between 10% to 30%.

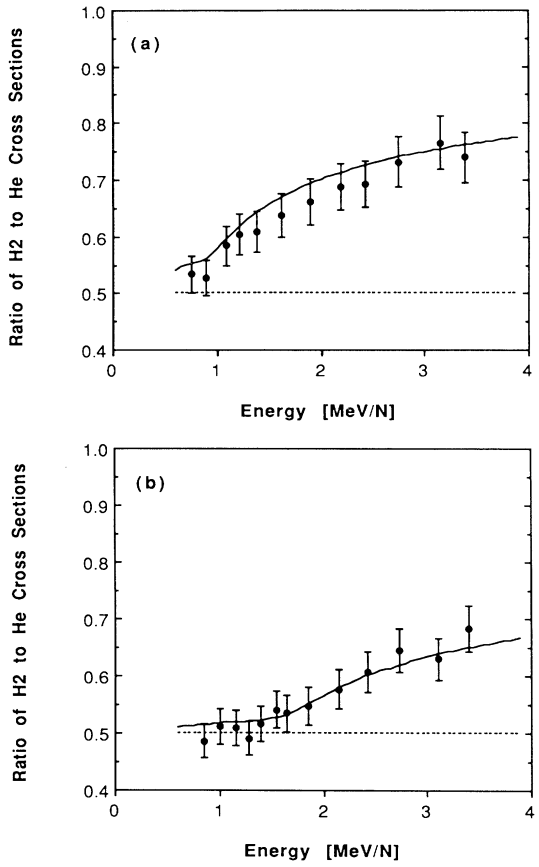

FIG. 3. Ratio of H_2 to He cross sections for (a) C^{5+} and (b) O^{7+}. Solid curves: screening-antiscreening ratios; dashed curves PWBA ratios.

difference between the two effective lengths is due to the difference in mass and viscosity between H_2 and He.) By making different assumptions about the gas flow, we estimate that the systematic error in the effective length is between 5% and 10%. The absolute error of our cross section measurement is therefore of the order of (10–15)%.

Figures 1 and 2 compare our experimental results and those of Refs. 8–10 and 15 with calculated cross sections for C^{5+} on H_2 and He and O^{7+} on H_2 and He. The solid curves are calculations based on Eq. (3) and include both screening and ionizing terms. The dashed curves represent the pure Born (bare target nucleus) calculations. The calculations for hydrogen have been performed for atomic hydrogen using the exact Bates-Griffing theory, but the calculations for He were computed by the Anholt prescription and have the unphysical kink at threshold, noted above. The calculations for hydrogen were multiplied by 2 in order to account for the hydrogen molecule. As a first approximation, this appears justified, since the screening-antiscreening effect contributes predominately at high momentum transfers (small impact parameters), where the H momentum wave functions are not disturbed much by molecular interactions.[8] A comparison of projectile ionization cross sections in H+H and $H+H_2$ collisions[16,17] shows that for $v/v_K > 0.5$ the aforementioned factor of 2 is approximately 1.7 (but, here, exchange effects are also important). We have also calculated the projectile ionization cross section for C^{5+} and O^{7+} on molecular hydrogen.[18] The target form factor for H_2 has been obtained by using the Weinbaum wave function[19] which takes into account the electron correlation within the H_2 molecule. Our preliminary results do not differ from the solid lines in Figs. 1(a) and 2(a) by more than 5%.

As expected, the difference between the curves representing screening-antiscreening and Born cross sections increases with energy and it does so relatively more for H_2 than for He. For H_2, our results for both C^{5+} and O^{7+} projectiles are in excellent agreement with the screening-antiscreening theory. Because of the size of the error, which is mainly systematic, the distinction be-

tween the two theories is not so clear in the case of $C^{5+}+He$. However, for $O^{7+}+He$ it appears that for higher energies the experimental data points fall closer to the screening-antiscreening line.

The ratio of the effective gas-cell lengths for H_2 and He has a much smaller systematic error than the individual absolute errors. Therefore, by taking the ratios of H_2 and He cross sections, the largest remaining sources of error are the statistical uncertainties and the effect of impurities in the target gases. In Fig. 3, we compare the ratios of our experimental results with the ratios of the two theoretical calculations for H_2 and He. The solid curve is the screening-antiscreening calculation and the dashed curve is the Born calculation. The ratio of the molecular H_2 to the atomic He Born cross section remains constant at 0.5, whereas the screening-antiscreening ratio increases markedly with energy. Our experimental values follow closely the screening-antiscreening curve.

In conclusion, we were able to demonstrate unambiguously the effect of the interaction between target and projectile electrons on the projectile K-shell ionization. Our experimental results show a clear deviation, by as much as 60%, from the Born calculations. Nevertheless, the inclusion of molecular effects, exchange effects, as well as second-order Born terms in the cross-section calculations appears desirable.

This work was supported in part by National Science Foundation Grant No. PHY 86-14650.

[1]D. R. Bates and G. Griffing, Proc. Phys. Soc. London, Sect. A **66**, 9611 (1953); **67**, 663 (1954); **68**, 90 (1955).

[2]J. H. McGuire, N. Stolterfoht, and P. R. Simony, Phys. Rev. A **24**, 97 (1981).

[3]T. Shirai, K. Iguchi, and T. Watanabe, J. Phys. Soc. Japan **42**, 238 (1977).

[4]R. Anholt, Phys. Lett. **114A**, 126 (1986).

[5]T. J. M. Zouros, D. H. Lee, and P. Richard, Phys. Rev. Lett. **62**, 2261 (1989).

[6]M. Schulz, J. P. Giese, J. K. Swenson, S. Datz, P. F. Dittner, H. F. Krause, H. Schöne, C. R. Vane, M. Benhenni, and S. M. Shafroth, Phys. Rev. Lett. **62**, 1738 (1989).

[7]R. D. DuBois and L. H. Toburen, Phys. Rev. A **38**, 3960 (1988).

[8]R. Anholt, X.-Y. Xu, Ch. Stoller, J. D. Molitoris, W. E. Meyerhof, B. S. Rude, and R. J. McDonald, Phys. Rev. A **37**, 1105 (1988).

[9]R. Hippler, S. Datz, P. D. Miller, P. L. Pepmiller, and P. F. Dittner, Phys. Rev. A **35**, 585 (1987).

[10]T. N. Tipping, J. M. Sanders, J. Hall, J. L. Shinpaugh, D. H. Lee, J. H. McGuire, and P. Richard, Phys. Rev. A **37**, 2906 (1988).

[11]N. F. Mott and H. S. W. Massey, *The Theory of Atomic Collisions* (Oxford Univ. Press, 1965), 3rd ed., Sec. XV. 1.

[12]N. Bohr, K. Dan. Vidensk. Selk. Mat.-fys. Medd. **18**, 144 (1948).

[13]Supplied by Matheson Gas Products, Newark, CA.

[14]S. Dushman, *Scientific Foundations of Vacuum Technique* (Wiley, New York, 1962), 2nd ed., Chapt. 2.

[15]S. A. Bowman, E. M. Bernstein, and J. A. Tanis, Phys. Rev. A **39**, 4423 (1989).

[16]A. B. Wittkower, G. Levy, and H. B. Gilbody, Proc. Phys. Soc. London **91**, 306 (1967).

[17]J. Hill, J. Geddes, and H. B. Gilbody, J. Phys. B **12**, 3341 (1979).

[18]Qiang Dai, W. E. Meyerhof, H.-P. Hüskötter, and J. H. McGuire (unpublished).

[19]S. Weinbaum, J. Chem. Phys. **1**, 593 (1933).